

CoRaiS: Lightweight Real-Time Scheduler for Multi-Edge Cooperative Computing

Yujiao Hu, *Member, IEEE*, Qingmin Jia, Jinchao Chen, Yuan Yao, Yan Pan, Renchao Xie, *Senior Member, IEEE*, F. Richard Yu, *Fellow, IEEE*

Abstract—Multi-edge cooperative computing that combines constrained resources of multiple edges into a powerful resource pool has the potential to deliver great benefits, such as a tremendous computing power, improved response time, more diversified services. However, the mass heterogeneous resources composition and lack of scheduling strategies make the modeling and cooperating of multi-edge computing system particularly complicated. This paper first proposes a system-level state evaluation model to shield the complex hardware configurations and redefine the different service capabilities at heterogeneous edges. Secondly, an integer linear programming model is designed to cater for optimally dispatching the distributed arriving requests. Finally, a learning-based lightweight real-time scheduler, *CoRaiS*, is proposed. *CoRaiS* embeds the real-time states of multi-edge system and requests information, and combines the embeddings with a policy network to schedule the requests, so that the response time of all requests can be minimized. Evaluation results verify that *CoRaiS* can make a high-quality scheduling decision in real time, and can be generalized to other multi-edge computing system, regardless of system scales. Characteristic validation also demonstrates that *CoRaiS* successfully learns to balance loads, perceive real-time state and recognize heterogeneity while scheduling.

Index Terms—Edge computing, Multi-edge cooperative computing, Deep learning, Real-time scheduling

I. INTRODUCTION

Edge computing brings computation and storage resources closer to the sources of data, facilitating the processing of client data at the network periphery while meeting stringent response time requirements. Some great progresses have been achieved, especially in the mobile edge computing [1], [2]. However, practical applications often reveal challenges. As shown in Fig. 1, each edge hosts a diverse set of services, and it typically serves multiple clients. The distribution of clients among edges exhibits non-uniformity, with variations in both the number of requests submitted by each client and the specific service they require. This complexity can potentially

Yujiao Hu, Qingmin Jia and Renchao Xie are with Future Network Research Center, Purple Mountain Laboratories, Nanjing 211111, China (email: huyujiao@pmlabs.com.cn, jiaqingmin@pmlabs.com.cn, renchao_xie@bupt.edu.cn). Jinchao Chen and Yuan Yao are with the School of Computer Science, Northwestern Polytechnical University, Xi'an 710029, China (email: cjc@nwpu.edu.cn, yaoyuan@nwpu.edu.cn). Yan Pan is with Science and Technology on Information Systems Engineering Laboratory, National University of Defense Technology, China (email:panyan@nudt.edu.cn) Renchao Xie is also with the State Key Laboratory of networking and Switching Technology, Beijing University of Posts and Telecommunications, Beijing 100876, China. F. Richard Yu is with the Department of Systems and Computer Engineering, Carleton University, Ottawa, Canada (e-mail: richard.yu@carleton.ca).

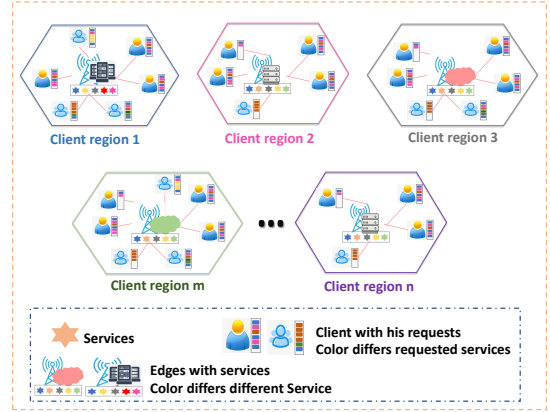


Fig. 1. The illustration of unbalanced workloads and resource utilization of edge computing.

degrade service quality, especially when an edge is inundated with an excessive number of client requests.

The multi-edge cooperative computing combining constrained resources of multiple edges into a powerful resource pool can provide more diversified services and ensure sufficient computing and storage resources. Therefore, it has higher probability to meet the requirements by computation-intensive and latency-critical requests, and improve the average utilization of edges and response time of requests. The edge-cloud system can be regarded as a special case of multi-edge cooperative computing, because the cloud can be considered as an edge with significantly enhanced computational capabilities.

Many researchers are interested in the multi-edge cooperation system, and have proposed some algorithms [3]–[8] to schedule independent requests and requests with logical execution order in the system. They usually make some hypotheses to support their research. Firstly, only CPU is configured on the edges, and the number of calculations required to respond to each request is known. With such two conditions, the response time of each request can be obtained by dividing the calculation number by the CPU frequency. Secondly, the request arrival patterns follow known probability distributions, such as poisson distribution, multinomial distribution, etc. With such assumption, many statistical theories and models can be applied to the multi-edge scheduling problems.

However, the assumptions contradict many practical situations. (i) *The heterogeneous edges are configured with various computing units, such as CPUs and GPUs.* Especially, with increasing requests related to deep learning accessing to edges,

it has become a major trend to deploy GPUs at edges. (ii) *It is difficult to estimate the calculation number required by requests.* Because, when the corresponding processing code is black-box, the calculation number cannot be predicted in advance; when the code is white-box but includes some loop operation and judgment statements, the timing of jumping out of loops and the judgment results are also unpredictable, which makes the calculation numbers impossible to be estimated. (iii) *The arrival pattern of requests is almost unpredictable.* Each client has its own unique request generation pattern. Though the pattern of a single client can be estimated, it is difficult to analyze the composite pattern of multiple clients. Besides that, another two phenomenons should be focused on, i.e. during the execution process of a service, it will occupy multiple resources such as CPU, GPU, and Memory simultaneously, and the quality of service (QoS) varies across edges¹.

Based on the analysis above, we can identify that the multi-edge cooperative scheduling faces three challenges. (i) *Multi-edge cooperative computing system state modeling:* The diverse hardware composition and different resource allocation schemes for services at edges pose a severe problem for modeling system state. The QoS of edges would not be fairly evaluated, unless the edges heterogeneity can be shielded and an unified QoS evaluation method can be built. Meanwhile, the system state that includes remaining resource of CPU/GPU/Memory at edges keeps changing as the arrival, running, and completion of requests. Dispatching requests to edges based on the perfect initial state, like traditional approaches, will make the scheduling solution deviate from the optimal at the current state. Therefore, it is challenging but necessary to build a system-level state model that supports edges unified modeling and perceives dynamic changes of resource states. (ii) *Multi-edge cooperative scheduling formulation:* Most previous theoretical models were designed based on probability distribution assumption of requests and single computing hardware assumption of edges [9], [10], which may not accurately reflect real-world application scenarios. Some learning-based approaches [4], [5] are also studied to optimize the scheduling behaviours on some specific datasets and specially constructed multi-edge network. However, the generalization ability² of the approaches is not good. Once the application and network environment change, a large amount of data (with expert knowledge sometimes) must be collected to retrain the scheduling model, while sometimes it is difficult to collect efficient data and expert knowledge. Therefore, a new mathematical formulation is required to reveal the essence of multi-edge cooperative scheduling problem and to guide scheduling algorithm research for requests with any arrival pattern. (iii) *Real-time scheduler designing:* The multi-

edge scheduling problem for multiple requests is essentially a combinatorial optimization problem with some constraints. The search space of such problem is huge and will grow as the number of edges and requests increase. Computing an optimal solution in the huge search space is theoretically time-consuming. The previous works usually took a long time to make the scheduling decision. However, in practice, only methods that support real-time scheduling can ensure the efficient operation of the multi-edge cooperative computing system.

To cope with the inherent challenges mentioned above, we first propose a system-level state evaluation model to express the service-oriented performance and workload of edges at any scheduling period. In this way, the important and differentiated performance characteristics closely related to edge scheduling are preserved, and the heterogeneous configuration of edges can be ignored when making scheduling decisions. Secondly, based on the system-level state evaluation model, we provide a new integer linear programming formulation for the multi-edge cooperation scheduling, which can be a good starting point to inspire solver searching or scheduling algorithms design. Finally, we propose *CoRaiS*, a reinforcement learning based lightweight real-time scheduler for multi-edge cooperative computing system. Given a high-level goal to minimize the response time of all requests, *CoRaiS* automatically learns a sophisticated system-level real-time scheduling policy. The policy can be directly generalized to other applications and multi-edge networks.

The main contributions of this paper can be summarized as follows.

- A system-level state evaluation model is built to capture important features closely related to scheduling across edges, including service-oriented performance feature and workload feature.
- The multi-edge scheduling problem is presented as a new integer linear programming formulation, which will support the designing and optimization of scheduling algorithms.
- A lightweight attention-based scheduler (*CoRaiS*) is proposed to minimize the response time over all requests distributed at edges. The scheduler can provide a high-quality near-optimal solution in real time, irrespective of request arrival patterns and system scales.

II. RELATED WORK

Existing works have explored the formulation and optimization of scheduling problems in the multi-edge or edge-cloud cooperative computing system and gotten some great contributions [11]–[13]. They generally divide dispatched requests into two categories: independent requests and requests with logical execution order, and then design scheduling algorithms respectively.

The efforts [3]–[5], [9], [10], [14]–[17] focus more on independent requests, as well as this paper. However, there are significant differences between these works and this paper in terms of modeling goal, problem settings and optimization approaches. The goal of works [3]–[5], [14] is to maximize

¹The Quality of Service (QoS) for a specific service exhibits variations among heterogeneous edges due to differences in their hardware configurations. Additionally, even among homogeneous edges with identical hardware configurations, the QoS may differ because they allocate different resources to the service. For instance, if two edges share the same hardware setup, one may assign a 2-core CPU to the service while the other allocates a 4-core CPU. As a result, the QoS of the service will vary between these two edges.

²Here the generalization ability refers to the pre-trained scheduling models can help make effective decisions on unseen applications and multi-edge networks.

the expected number of requests served per slot with different assumptions. The work [3], [14] assume that the computation requirement and average arrival rate of requests are known, formulates the problem as an integer linear program and prove the problem is generally NP-hard. A heuristic approximation algorithm based on linear program relaxation and rounding is proposed to solve the problem as well. The work [4] builds their own experiment environment that consists of some physical servers and leased clouds, and proposes a coordinated multi-agent actor-critic algorithm for decentralized request dispatch. The algorithm is evaluated on real-world workload traces from Alibaba. Another learning-based scheduling model *EdgeMatrix* is presented to maximize the throughput while guaranteeing various Service-Level-Agreement priorities in the work [5], where a networked multi-agent actor-critic algorithm to customize resource channels is proposed to improve the system's stability. The work [15] formulates a request routing problem under the assumptions of computation capacity (i.e. maximum frequency) of a single CPU in the multi-cell mobile edge computing networks, and proposes a randomized rounding algorithm to minimize the load to cloud. The work [9] assumes that the request arrival at each edge is a Poisson process, the computation requirements (in CPU cycle) of requests follow exponential distribution, and the cloud always has enough computation capacity to provide near-zero computing delay. The work [10] assumes the dynamic arrival of computation requests can be approximated as Poisson process, and the request requires the computing support by a random number of CPU cycles with a finite mean value. The authors transform the scheduling problem into a cooperative queueing game approach to minimize the expected cost of each individual edge server. The works [16], [17] attach to the response time of each request a weight to indicate its latency sensitivity and introduce a machine-dependent processing time in each server. Then the works propose an online scheduling framework based on question and answer (Q&A) mode to minimize the total weighted response time over all requests.

There are some other progresses on dispatching requests with logical execution order [6], [7], [18]–[20]. The dependencies among such requests are usually formulated as directed acyclic graphs (DAGs), and the dependency-aware requests scheduling problems are also known as DAG scheduling problem. The work [18] proposes *Decima* that develops new representations for requests' dependency graphs and adopts scalable reinforcement learning models to learn work-load-specific scheduling algorithms without any human instruction, in order to minimize average request completion time. The paper [19] allocates computing devices to continuous data flows in a large distributed system, through presenting a graph-aware encode-decoder framework to learn a generalizable resource allocation strategy. The works [6], [7], [20] present how to optimize device placement for training deep neural networks (DNN). The architecture of a DNN model can take as a DAG, and the device placement for DNN is to specify how each operation in a DNN model should be matched to the heterogeneous CPU and GPU devices. The [20] presents a sequence-to-sequence model that learns to optimize device placement for TensorFlow computational graphs. *Spotlight* is

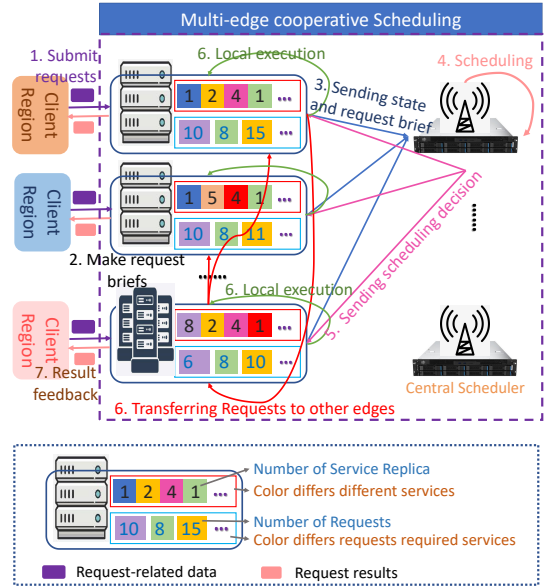


Fig. 2. Scheduling processes in multi-edge cooperative computing

proposed [6] to find an optimal device placement for training DNNs. *Spotlight* models the problem as a Markov decision process with multiple stages, and uses a new reinforcement learning algorithm based on proximal policy optimization. A two-level hierarchical model [7] realizes device placement for a neural network with tens of thousands of operations.

In general, the scheduling problem can be taken as a combinatorial optimization problem under some constraints and is proved to be NP-hard. In recent years, designing algorithms to quickly solve combinatorial optimization problems has attracted much attention, and some achievements have been made. The works [21], [22] design learning-based models to solve traveling salesman problems (TSP). The advances [23]–[25] learn policies for vehicle routing problems (VRP). The works [26] propose reinforcement learning based models to solve multiple TSP. The progresses [27], [28] present common frameworks for combinatorial problems. Solutions for mixed integer programming (MIP) are proposed as well [29], [30].

III. SYSTEM MODEL AND PROBLEM FORMULATION

A. Multi-edge Cooperative Scheduling Processes

The multi-edge cooperative computing system consists of a set of network edges $\mathcal{E} = \{e_n\}_{n=1}^N$, and can provide diverse services $\mathcal{S} = \{s_k\}_{k=1}^K$. Each edge is under the exclusive management of a single central scheduler, effectively eliminating the possibility of ambiguous scheduling decisions. Furthermore, every edge within the system willingly collaborates with others and entrusts the central scheduler's decision-making efficacy. Consequently, each edge actively accepts transmitted requests without rejection. This collective commitment ensures a seamless and efficient process, contributing to the overarching goal of achieving timely completion of all tasks. The processes of multi-edge cooperative scheduling are shown in Fig. 2. Before describing the detail processes, we first explain some concepts used in the scheduling process as follows.

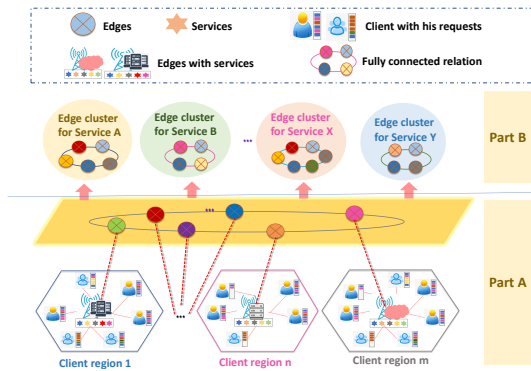


Fig. 3. Multi-edge cooperative computing system modeling. *Part A*: The edges are physically interconnected. Each edge has its dedicated client region and the services deployed on each edge operate independently. *Part B*: The multi-edge cooperative computing system is decomposed into multiple independent service-oriented subsystems, where the edges with same service are grouped.

Request: A request usually consists of description text and physical input data. The description text describes the required service, the client ID, etc. Input data is the data to be processed. For example, an image classification request should explain which classifier is required in the description text, and upload the related images as input data.

Request brief: It is a data package that only has some description information of request, without detailed input data. For example, the brief of an image classification request records the size of images and required classifier, and does not include the content of images. By introducing request brief, the data packages used to make scheduling decisions become very small, which would significantly reduce the communication delay among edges and central controller.

Scheduling decision: It contains the information which edge the requests would be executed at. The edges must obey the decision to locally respond to the requests or transfer the requests to other edges.

Then as shown in Fig. 2, the scheduling processes involve seven steps. (i) Clients submit requests and related data to edges. (ii) Edges receive requests and create a request brief for each of them. (iii) Edges submit current service capacity information and the briefs to central controller (CC). (iv) CC makes a scheduling decision based on edge status and request briefs, and designated scheduling algorithms. (v) CC informs edges about the decision, where the execution edge for each request is decided. (vi) Based on the decision, edges determine whether to locally respond to the requests or transmit them to other edges with the relevant data. (vii) The edges feed back the computing results to clients.

B. System Scheduling Decomposition

As the decomposition principle illustrated in Fig. 3, we decompose the multi-edge cooperative system into multiple service-oriented subsystem, i.e. $\{SR_k\}_{k=1}^K$, where $SR_k = \{e_{k1}, e_{k2}, \dots, e_{kn'}\}$ and e_{ki} denotes the i^{th} edge with service s_k . With the decomposition, our focus can then shift towards addressing scheduling problem within each individual subsystem, since the process of scheduling over the whole multi-edge system can be decomposed into scheduling on each SR_k .

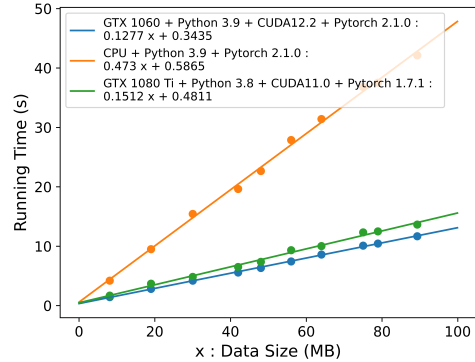


Fig. 4. The linear relationship between running time and the size of data packets for *Model Soups* [31] on heterogeneous devices. Points are actual statistical data, while lines are function relationships fitted based on the data.

For the sake of clarity in the following discussions, we omit explicitly declaring the s_k -oriented. However, it's important to understand that all the operations described can be applied into any service-oriented subsystem.

C. System-level State Evaluation Model

The system-level state evaluation model is inspired by some observations. The first key observation is that there are many popular artificial intelligence services, such as image classification and object detection, exhibiting a functional relationship between their response time and the size of the data packets to be processed. We select the most advance image classification model *Model Soups* [31] as an example to illustrate the observation, and visualize the relationship of *Model Soups* in Fig. 4. In Fig. 4, we can observe that the running time and data size of *Model Soups* is linearly correlated, and the coefficients of the linear function are related to the configuration of computing devices. The most popular object detection model, *YOLOv6* [32], [33] also cares about the computation efficiency. They reports the linear relationship between running time and data size for different vision of *YOLOv6* when inferring on Tesla T4. Please note, in this paper, we refer to services that have a functional relationship between runtime and data size as *ideal services*, and our study primarily focuses on this category. The second observation is that many advanced technologies, such as *Docker* and *Kubernetes*, empower one service to create multiple independent replicas on a single device and enable the service to specify the required resources. This reservation mechanism ensures that the resources allocated to each service replica are safeguarded against preemption by other processes, thereby stabilizing the QoS of the service.

Based on these observations, we build our system-level state evaluation model. The model consists of two parts: *service-oriented performance estimation* and *service-oriented workload evaluation*.

1) *Service-oriented Performance Estimation*: Two indicators are used to consistently evaluate the service-oriented performance of edges, that are *computation time estimation function* ($\phi(x)$) and *service replica numbers* (ζ). $\phi_i(x)$ is a function that depicts the relationship between the response

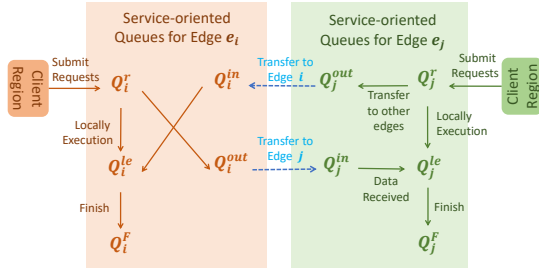


Fig. 5. Illustration of the state transition of requests across queues. Clients submit requests to Q_i^r . After receiving the scheduling decision, requests that will be locally executed are transferred from Q_i^r to Q_i^{le} , and requests that will be executed on other edges are transferred from Q_i^r to Q_i^{out} . The requests that are transferred from other edges are saved in Q_i^{in} . Once the related data of requests in Q_i^{in} are received, the requests are transferred from Q_i^{in} to Q_i^{le} . If the requests are completed, then they are transferred from Q_i^{le} to Q_i^f .

time and the size of data packets to be processed at edge e_i , with x denotes the size of the data packets. $\phi_i(x)$ can be approximated by fitting the relationship between data volume and the actual processing time of historical requests, like the fitting operation in Fig. 4. There are some tools that can help establish the relationship, such as *numpy.polyfit* and *scipy.optimize.curve_fit*. The hardware configuration also has a significant impact on the execution efficiency, causing $\phi(x)$ to vary across different edges. Fig. 4 illustrates the impact as well. Therefore, when establishing the relationship, only local historical data can be selected. ζ_i refers to the replica number of the service on edge e_i , which is a predefined system-level parameter to support service parallels. A larger ζ_i indicates edge e_i can deal with more requests in parallel.

By defining $\phi(x)$ and ζ , we can focus on considering the primary performance factors of edges while formulating multi-edge cooperative scheduling problem and designing algorithms, and ignore the secondary factors (the heterogeneous hardware configuration and various resource allocation mechanism to services at edges). Furthermore, with $\phi_i(x)$, we can predict response times on any edge by inputting the request's data size. This eliminates the need to analyze black box or white box code to obtain the necessary computation numbers for the request and restricts the computing device to the CPU.

2) *Service-oriented Workload Evaluation*: We design service-oriented queue models for edge e_i to save requests that are at different status, including Q_i^r for requests that are waiting for scheduling, Q_i^{le} for requests that will be executed locally, Q_i^{out} for requests that will be transmitted to other edges, Q_i^{in} for requests that will be transferred in from other edges and Q_i^f for requests that have been completed. The state transition of requests across queues is presented in Fig. 5.

When evaluating the workload of edge e_i , we focus on the requests in Q_i^{le} and Q_i^{in} , because only requests in these two queues will make use of the local resources of edge e_i . Three features are introduced to evaluate the workloads, including required computing time to complete requests in Q_i^{le} (referred to as c_i^{le}), required data transmission time for requests in Q_i^{in} (referred to as t_i^{in}), and required computing time to complete requests in Q_i^{in} (referred to as c_i^{in}).

c_i^{le} , t_i^{in} and c_i^{in} can be evaluated in customized mathematical

approximation models. In this paper, we compute them by (1), (2) and (3) respectively. r refers to a request. α_r refers to the data size of request r . β_r^i denotes the distance between the source edge of r and edge e_i . C_t is a constant to represent the transmission speed for unit data through unit distance. In (1) and (3), we average the computation time required to complete all tasks across multiple copies. As for (2), we make two assumptions based on experience to predict required data transmission time. Firstly, the data transmission time is positively correlated with both data size and transmission distance. Secondly, edges can simultaneously receive data sent by other edges from different ports.

Evaluating the workload before each scheduling operation allows us to obtain the real-time service capacity of edge e_i . This real-time system state knowledge is instrumental in making well-informed scheduling decisions.

$$c_i^{le} = \frac{\sum_{r \in Q_i^{le}} \phi_i(\alpha_r)}{\zeta_i} \quad (1)$$

$$t_i^{in} = \max_{r \in Q_i^{in}} C_t \alpha_r \beta_r^i \quad (2)$$

$$c_i^{in} = \frac{\sum_{r \in Q_i^{in}} \phi_i(\alpha_r)}{\zeta_i} \quad (3)$$

D. Problem Formulation

In this paper, the multi-edge cooperative scheduling problem in each SR_k has similar formulation. We firstly define some parameters to formulate the SR_k as $CoMEC = (\mathcal{E}, \mathcal{W}, \mathcal{V}, \mathcal{P}, \mathcal{I})$. $\mathcal{E} = \{e_q\}_{q=1}^Q$ is a set of network edges where s_k is deployed, $|\mathcal{E}| = Q$ is the number of edges. \mathcal{W} is a $Q \times Q$ matrix that specifies the data transmission distance between any pair of edges, i.e. the entry of \mathcal{W} at the i^{th} row and j^{th} column, denoted by $w_{ij} \in \mathbb{R}_+$, is the time cost to transmit one unit data from e_i to e_j . For disconnected e_i and e_j , $w_{ij} = +\infty$. $\mathcal{V} = \{\phi_q\}_{q=1}^Q$ is a set of functions and ϕ_q represents computation time estimation function of e_q (explained in the section III-C1). \mathcal{P} is a Q -dimensional vector as well. p_i denotes the replica numbers of s_k at e_i . \mathcal{I} is a $N \times 3$ matrix that specifies the current workload evaluation of edges. The entry of \mathcal{I} at q^{th} row, denoted as I_q , represents the workload evaluation of e_q . $I_q = (c_q^{le}, c_q^{in}, t_q^{in})$ (the definitions are explained in the section III-C2).

The requests distributed in SR_k can be modeled as $CoR = (\mathcal{R}, \mathcal{L}, \mathcal{F}, \mathcal{D})$. $\mathcal{R} = \{r_z\}_{z=1}^Z$ is a set of requests that require s_k , $|\mathcal{R}| = Z$ is the number of requests. \mathcal{L} is a $Z \times Q$ matrix, the entry l_{zq} represents whether r_z is located at e_q before scheduling, if yes, $l_{zq} = 1$, else, $l_{zq} = 0$. $\mathcal{F} = \{f_z\}_{z=1}^Z$ is a set that records the size of input data for all $r_z \in \mathcal{R}$. \mathcal{D} keeps the practical related data of requests.

Given $CoMEC$ and CoR , let $\mathcal{X} \in \{0, 1\}^{Z \times Q}$ be a permutation matrix. For $\forall x_{zq} \in \mathcal{X}$, $x_{zq} = 1$ represents r_z is dispatched to e_q . Then the objective function of multi-edge cooperative scheduling problem can be formulated as (4). The parameter T_q in (4) denotes the required time to complete all requests that are scheduled to e_q as \mathcal{X} . (4) indicates that the purpose is to get a \mathcal{X} that can minimize the response time over

TABLE I
THE DEFINITIONS OF PRIMARY NOTATIONS

Notation	Definition
r_z	The request z
e_q	The edge q
s_k	The service k
l_{zq}	Whether r_z is located at e_q . $l_{zq} \in \{0, 1\}$
x_{zq}	Whether r_z is dispatched to e_q . $x_{zq} \in \{0, 1\}$
f_z	The input data size of r_z .
$\phi_q(f_z)$	The computation time to deal with data of r_z at e_q .
p_q	The replica number of s_k at e_q
c_q^{le}	The computation time to complete backlogs in Q_q^{le} .
c_q^{in}	The computation time to complete backlogs in Q_q^{in} .
w_{nq}	The transmission distance e_n and e_q .
C_t	A constant to represent the transmission speed for unit data through unit distance.
t_q^{in}	The remaining transmission time of backlogs in Q_q^{in} .
$[Z]$	$\{1, 2, \dots, Z\}$. Z denotes the number of requests.
$[Q]$	$\{1, 2, \dots, Q\}$. Q denotes the number of edges.

all edges and all requests. T_q in (4) can be computed by (5)-(9) with constraints (10) and (11). The definitions of primary notations in the formulation are summarized in Table I.

$$obj. \min_{\mathcal{X}} \max_{e_q \in \mathcal{E}} T_q \quad (4)$$

$$\mu_q = \frac{\sum_{z \in [Z]} l_{zq} x_{zq} \phi_q(f_z)}{p_q} + c_q^{le}, \quad \forall q \in [Q] \quad (5)$$

$$\eta_q = \frac{\sum_{z \in [Z]} (1 - l_{zq}) x_{zq} \phi_q(f_z)}{p_q} + c_q^{in}, \quad \forall q \in [Q] \quad (6)$$

$$v_q = \max_{z \in [Z]} x_{zq} f_z \left(\sum_{n \in [Q]} l_{zn} w_{nq} \right), \quad \forall q \in [Q] \quad (7)$$

$$\kappa_q = \max(C_t v_q, t_q^{in}) \quad (8)$$

$$T_q = \max(\kappa_q, \mu_q) + \eta_q, \quad \forall q \in [Q] \quad (9)$$

$$s.t. \sum_{q \in [Q]} x_{zq} = 1, \quad \forall z \in [Z] \quad (10)$$

$$x_{zq} \in \{0, 1\}, \quad \forall z \in [Z], \forall q \in [Q] \quad (11)$$

To be specific, (5) predicts the required computing time to complete all requests that will be executed locally, including previous backlogs and new requests scheduled as \mathcal{X} . (6) evaluates the required computing time to complete all requests that are transferred from other edges to e_q , taking into account both backlogs and new requests scheduled as \mathcal{X} . (7) predicts the required longest transmission time for data of new requests that are transferred from other edges to e_q as \mathcal{X} , since multiple edges transmitting data to the same edge in parallel is allowed in our multi-edge cooperative computing system. Considering that the data of backlogs may haven't been transmitted to e_q , we design (8) to estimate the maximum transmission time for all requests that are transferred from other edges to e_q , including both backlogs and new requests scheduled as \mathcal{X} , through max operation over $C_t v_q$ and t_q^{in} . Furthermore, due to data transmission and local computing can run simultaneously, and the requests in Q_q^{in} cannot be

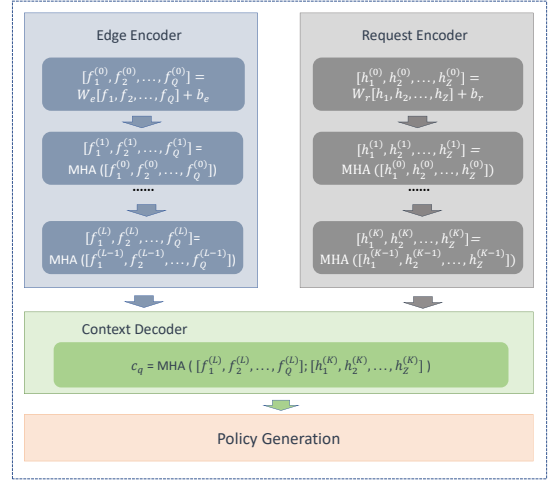


Fig. 6. Matching-on-demand architecture of *CoRaiS*

executed until all relevant data has been received by e_q , we design (9) to predict the required response time to complete all requests that are scheduled to e_q as \mathcal{X} , including backlogs and new requests as well. Here max operation is used to select the case that consumes longer time. While computing a feasible \mathcal{X} , constraints (10) and (11) must be met to ensure all requests can be scheduled to only one available edge.

Throughout the system's operation, there will be multiple task scheduling rounds. In each scheduling round, the formulation can be utilized to obtain the optimal solution \mathcal{X} based on the current system state *CoMEC* and request state *CoR*.

IV. LIGHTWEIGHT REAL-TIME SCHEDULER DESIGN

The scheduling problem has been represented as an integer linear programming formulation. There have been some solvers, such as *Gurobi* and *Cplex*, which can accurately solve such problems. However, the search space of multi-edge cooperative scheduling problem is Q^Z , and it will significantly grow as the number of edges or requests increases. Therefore, getting the optimal solution is theoretically time-consuming. It is necessary to design a novel algorithm that can provide a high-quality solution within a short and predictable time. This paper proposes a lightweight attention-based scheduler called *CoRaiS*, and combines it with reinforcement learning to automatically learn a great policy that helps produce a high-quality scheduling decision in real time.

A. Architecture of *CoRaiS*

CoRaiS adopts matching-on-demand (MoD) architecture that consists of two alignment modules (edge encoder and request encoder) and one matching module (context decoder), as presented in Fig. 6. The alignment modules are used to align specific features of heterogeneous edges through multi-dimensional information exchange. Specifically, the edge encoder embeds and aligns the performance information of edges through multi-head attention mechanism (MHA), and captures the service capacity of multi-edge system by max pooling; the request encoder has similar function with edge encoder, but

works on the requests contexts, i.e. request encoder focuses on capturing and aligning the requirements of requests through MHA, and mastering the global request features by max pooling. The matching module (context decoder) associates the capacity of multi-edge computing system with the requirements of requests through aggregating edges embeddings and requests embeddings, and produces scheduling policies to realize edge matching based on the demands of request.

Edge encoder: It is a module to embed edge features. At the beginning of training, input features of edges \mathbf{f} are initialized based on the current edge states. To be specific, the input features \mathbf{f}_q of e_q include (i) coordinates (x_q, y_q) ; (ii) the coefficients of ϕ_q and replica numbers ζ_q ; (iii) workload evaluation vector I_q , and $I_q = (c_q^{le}, c_q^{in}, t_q^{in})$. The encoder computes initial d_h -dimensional edge embeddings $\mathbf{f}_q^{(0)}$ through a learnable linear projection with parameters \mathbf{W}_e and \mathbf{b}_e : $\mathbf{f}_q^{(0)} = \mathbf{W}_e \mathbf{f}_q + \mathbf{b}_e$. Then the embeddings are updated through L attention layers, which is motivated by Transformer [34] and Attention Model [24]. Each layer consists of two sublayers: a multi-head attention layer (MHA) and an edge-wise fully connected layer (FC). A skip-connection and batch normalization (BN) are also used at each sublayer. The operations are formulated as (12), where $\mathbf{f}_q^{(l)}$ denotes the produced edge embedding by layer $l \in \{1, \dots, L\}$.

$$\begin{aligned} \mathbf{f}_q^{(l)} &= \text{BN}^l(\mathbf{f}_q^{(l-1)} + \text{MHA}_e^l(\{\mathbf{f}_q^{(l-1)}\}_{q=1}^Q)) \\ \mathbf{f}_q^{(l)} &= \text{BN}^l(\mathbf{f}_q^{(l)}, \text{FC}_e^l(\mathbf{f}_q^{(l)})) \end{aligned} \quad (12)$$

Request Encoder: It has similar architecture and operations with *edge encoder* to embed request features. But the learnable parameters are different. The initial feature h_z of r_z includes (i) coordinates of the source edge of r_z ; (ii) input data size of r_z . The initial features $\mathbf{h}_z^{(0)}$ are initialized to a d_r -dimensional embeddings by linear projection as (13). Following that, K attention layers are used to update request embeddings. The operations are presented as (14), where MHA_r^k and FC_r^k are the parameters that are used to embed requests features. The operations of MHA_r^k are similar with them in MHA_e^l .

$$\mathbf{h}_z^{(0)} = \mathbf{W}_r \mathbf{h}_z + \mathbf{b}_r \quad (13)$$

$$\begin{aligned} \mathbf{h}_z^{(k)} &= \text{BN}^k(\mathbf{h}_z^{(k-1)} + \text{MHA}_r^k(\{\mathbf{h}_z^{(k-1)}\}_{z=1}^Z)) \\ \mathbf{h}_z^{(k)} &= \text{BN}^k(\mathbf{h}_z^{(k)}, \text{FC}_r^k(\mathbf{h}_z^{(k)})) \end{aligned} \quad (14)$$

Context decoder: The system context comes from the edge embeddings $\{\mathbf{f}_q^{(L)}\}_{q=1}^Q$ and request embeddings $\{\mathbf{h}_z^{(K)}\}_{z=1}^Z$. Inspired by [22], [35], [36], this paper captures global features $\hat{\mathbf{f}}$ and $\hat{\mathbf{h}}$ by max pooling operation over $\{\mathbf{f}_q^{(L)}\}_{q=1}^Q$ and $\{\mathbf{h}_z^{(K)}\}_{z=1}^Z$, respectively. Then the new context embedding \mathbf{c}'_q is produced by MHA_c which has M heads. The computation process through MHA_c is shown as (15), where $[\cdot, \dots, \cdot]$ is the horizontal concatenation operator, $d_y = \frac{d_r}{M} = \frac{d_h}{M}$, \mathbf{c}'_q is the

embedding after single attention, and \mathbf{c}_q is the final multi-head attention value for context embedding.

$$\begin{aligned} \mathbf{f}_{(c)q} &= [\hat{\mathbf{f}}, \hat{\mathbf{h}}, \mathbf{f}_q^{(L)}] \\ \mathbf{x}_q &= \mathbf{W}_c^x \mathbf{f}_{(c)q}; \quad \mathbf{y}_z = \mathbf{W}_c^y \mathbf{h}_z^{(K)}; \quad \mathbf{v}_z = \mathbf{W}_c^v \mathbf{h}_z^{(K)} \\ u_{qz} &= \frac{\mathbf{x}_q^T \mathbf{y}_z}{\sqrt{d_y}}; \quad a_{qz} = \frac{e^{u_{qz}}}{\sum_{z=1}^Z e^{u_{qz}}} \\ \mathbf{c}'_q &= \sum_{z=1}^Z a_{qz} \mathbf{v}_z; \quad \mathbf{c}_q = \sum_{i=1}^M \mathbf{W}_{c,i} \mathbf{c}'_q \end{aligned} \quad (15)$$

The MHA operation in *context embedding* is similar with it in *edge encoder* and *request encoder*, but replacing $\mathbf{f}_{(c)q}$ with $\mathbf{f}_q^{(l-1)}$ ($\mathbf{h}_z^{(k-1)}$) in *edge encoder* (*request encoder*).

Policy generation: The policy is generated by collecting importance of edges for one request r_z as (16). imp_{qz} denotes the importance of e_q for r_z . C is a constant. To evaluate the probability of edges getting the privilege, *softmax* is introduced over all edges for each request as (17), where a_{qz} specifies the probability of e_q responding to r_z .

$$\begin{aligned} \mathbf{p}\mathbf{x}_q &= \mathbf{W}_{px} \mathbf{c}_q; \quad \mathbf{p}\mathbf{y}_z = \mathbf{W}_{py} \mathbf{h}_z^{(H)}; \\ u_{qz} &= \frac{\mathbf{p}\mathbf{x}_q^T \mathbf{p}\mathbf{y}_z}{\sqrt{d_{py}}}; \quad \text{imp}_{qz} = C \tanh(u_{qz}) \end{aligned} \quad (16)$$

$$a_{qz} = \frac{e^{\text{imp}_{qz}}}{\sum_{q=1}^Q e^{\text{imp}_{qz}}} \quad (17)$$

B. Training CoRaiS

The scheduling probability distribution $p_\theta(\pi) = \{a_{qz}\}_{q \in [Q], z \in [Z]}$ is produced by *CoRaiS*, from which we can sample a scheduling decision π . In order to train *CoRaiS*, we define the expectation of the maximum response time of all requests over edges as loss function: $\mathcal{L}(\theta|g) = \mathbb{E}_{p_\theta(\pi)}[L(\pi)]$. Given π , $L(\pi) = -\hat{u}^\pi$ is computed according to (18) and (19). Firstly, a local reward u_q is estimated by (18), where RL_q^π denotes the set of requests to be executed locally and RT_q^π includes requests that are transferred from other edges to e_q , based on the decision π . $Y(\varpi_m, e_q)$ is a function to compute the transmission distance between the source edge ϖ_m and the execution edge e_q of r_m . The connotation of each equation in (18) is similar with (5)-(9). Then the global reward is formulated as (19).

$$\begin{aligned} \mu_q &= \frac{\sum_{r_m \in RL_q^\pi} \phi_q(f_m)}{\zeta_q} + c_q^{le} \\ \eta_q &= \frac{\sum_{r_m \in RT_q^\pi} \phi_q(f_m)}{\zeta_q} + c_q^{in} \end{aligned} \quad (18)$$

$$\begin{aligned} \kappa_q &= \max\left\{ \max_{r_m \in RT_q^\pi} f_m Y(\varpi_m, e_q), t_q^{in} \right\} \\ u_q^\pi &= -(\max(\mu_q, \kappa_q) + \eta_q) \\ \hat{u}^\pi &= \min_{e_q \in \mathcal{E}} u_q^\pi \end{aligned} \quad (19)$$

We use S -samples batch reinforcement learning (RL) and gradient descent [26] to optimize \mathcal{L} , since the S -samples batch gradient descent replacing the one-sample approximation in

training realizes more accurate estimation of the policy, decreases training variance and speeds up convergence. Meanwhile, to encourage *CoRaiS* to sufficiently explore the huge search space, we add an extra entropy loss $H(\theta)$, computed as (20). Then the optimization function can be formulated as (21), where D is the training data set, C_1 and C_2 are the coefficients.

$$H_{\theta}(g) = - \sum_{z=1}^Z \sum_{q=1}^Q a_{qz}(\theta) \log a_{qz}(\theta) \quad (20)$$

$$\begin{aligned} A(\pi_s) &= L(\pi_s) - \frac{1}{S} \sum_{i=1}^S L(\pi_i) \\ \mathcal{L}(\theta|D) &= \mathbb{E}_{g \sim D} (C_1 \sum_{s=1}^S \log p_{\theta}(\pi_s|g) A(\pi_s) \\ &\quad - C_2 H_{\theta}(g)) \end{aligned} \quad (21)$$

We generate synthetic data to build the training dataset D for some reasons. Firstly, even though Alibaba has provided the most prominent cluster dataset, *CoRaiS* cannot be trained using the dataset, because majority of services in the dataset are related with online shopping applications, which are not ideal services³ focused on in this paper. Only a few offline services may meet the characteristic of ideal services, but it is difficult to separate them from the dataset. Moreover, the dataset is closely tied to the specific multi-edge cooperative system built by Alibaba, hence, there is uncertainty regarding whether a scheduling policy trained on the dataset would perform well on other multi-edge systems. Secondly, no other datasets containing enough data can be used to train *CoRaiS*. Thirdly, when generating synthetic data, we can vary the multi-edge cooperative environments and the scheduled services. In this way, the synthetic dataset becomes more comprehensive and better supports *CoRaiS* in learning a more versatile scheduling policy. To introduce variation of multi-edge cooperative environments, we can vary the number and position of heterogeneous edges, as well as the number of requests submitted to the each edges. To diversify the scheduled services, we can establish different computation time estimation function and service replica numbers (explained in Section III-C1) to express runtime performance of different services.

C. Decode Strategies of *CoRaiS*

Two decoding strategies are proposed for *CoRaiS* to generate an effective scheduling decision.

- Greedy decoding: according to the generated policy of *CoRaiS*, the best execution edge for each request is always selected. That is, for request r_z , its execute edge e_q is selected by $q = \arg \max_k \{a_{kz}\}_{k=1}^Q$.
- Sampling decoding: for request r_z , multiple edge selections can be sampled based on multinomial probability distribution over the policy $\{a_{qz}\}_{q=1}^Q$, and the best

³We explain *ideal services* in Section III-C. *Ideal services* refers to services that has a functional relationship between running time and data size.

one is reported. A complete scheduling decision entails execution edge selections of requests in the multi-edge computing system.

V. EVALUATION

To demonstrate that *CoRaiS* is able to learn a strong policy and give a real-time decision for the multi-edge scheduling problem, we designs three experiments: conventional test, generalization test, and characteristic validation. Conventional test refers to evaluating the performance of *CoRaiS* on a dataset that matches the same scale⁴ as the one it was trained on. Generalization test refers to evaluating the performance of *CoRaiS* on a dataset that has large scale than the one it was originally trained on. Characteristic validation is used to assess whether *CoRaiS* can perceive the workload and heterogeneity of edges, and autonomously implement load balancing.

A. Experiment Descriptions

Instance generation The training and testing datasets are generated as the same rules. Given the number of edges and requests (Q, Z) , for each edge e_q , the coordinates are randomly sampled under the uniform distribution in $(0, 1)^2$; the supported maximum service replica number rn_q is randomly sampled in $\{1, 2, 3, 4\}$. The functional relationship between computing time and the size of input data packets is modeled as linear functions⁵ for all edges during simulations. Moreover, to represent the heterogeneity across edges, different coefficients are randomly sampled from a uniform distribution within the range $(0, 1)$.

To make *CoRaiS* can learn to adopt to any initial system-level state, we randomly generate some requests as backlogs for each edge while generating training dataset and testing dataset. The number of backlogs in Q_q^{le} and Q_q^{in} of edge e_q are randomly sampled from $(0, 100)$. For any backlog r_x in Q_q^{le} , its input data size f_x is uniformly sampled from $(0, 1)$. For any backlog r_k in Q_q^{in} , its source edge ϖ_k is sampled from $[Q] - \{q\}$, and its input data size f_k is uniformly sampled from $(0, 1)$. With these backlogs, the service-oriented workload evaluation are carried out as (1)-(3).

For any new request r_z that will be scheduled in current period, its source edge ϖ_z is sampled from $[Q]$, and the size of related input data f_z is uniformly sampled from $(0, 1)$.

Hyperparameters Learnable parameters are initialized as $\text{Uniform}(-1/\sqrt{d}, 1/\sqrt{d})$, with d is the input dimension; learning rate $lr = 1e - 5$; batch size is 128, $S = 64$ while using S -samples batch RL; $C_1 = 10$ and $C_2 = 0.5$. The *edge encoder* and *request encoder* have $L = 5$ and $K = 3$ attention layers, respectively. **MHA** and **FC** in two embedding modules same structure, i.e. **MHA** has 8 heads, **FC** has one hidden sublayer with dimension 512 and ReLU activation.

⁴In this paper, the *scale* of dataset refers to the size of the multi-edge cooperative system, including the number of edges in the system and the number of requests submitted to it.

⁵Without loss of generality, we model the relationship using the linear functions. But in practical, other relationships, such as quadratic function, are allowed to train *CoRaiS*.

TABLE II
CONVENTIONAL TEST RESULTS

(*Time(s)* AND *Gap*: THE LOWER THE BETTER. *EN* AND *RN* DENOTE THE NUMBER OF EDGES AND NEW REQUESTS RESPECTIVELY. 1K=1000. (*x%*) IN THE COLUMN OF *Time* INDICATES *x%* OF TEST INSTANCES ARE RESOLVED. (*y*) IN THE COLUMN *Gap* INDICATES THAT ONLY SUCCESSFULLY RESOLVED INSTANCES ARE COUNTED WHILE COMPUTING QUALITY DIFFERENCE.)

Method	EN=5, RN=50		EN=10, RN=50		EN=5, RN=100		EN=10, RN=100	
	Time(s)	Gap	Time(s)	Gap	Time(s)	Gap	Time(s)	Gap
Gurobi(10s)	0.3592	1	0.3473	1	0.6542	1	3.4865	1
Gurobi(1s)	0.3252	1	0.3373	1	0.1252	1.0001	0.4921	1.0001
Local	-	2.1712	-	2.8032	-	1.8594	-	2.7055
Random(1)	-	2.1987	-	2.8023	-	1.9198	-	2.759
Random(100)	-	1.2916	-	1.8148	-	1.2732	-	1.7422
Random(1k)	-	1.2916	-	1.6282	-	1.1863	-	1.5854
FC1-CoRaiS(greedy)	0.0050	3.1129	0.0052	4.638	0.0052	3.346	0.0052	5.3293
FC2-CoRaiS(greedy)	0.0051	4.0758	0.0051	5.7307	0.0052	4.4914	0.0051	7.8728
FC3-CoRaiS(greedy)	0.0051	4.0758	0.0052	5.7307	0.0053	4.4914	0.0051	7.8728
CoRaiS(greedy)	0.0051	1.0783	0.0052	1.0953	0.0052	1.0450	0.0051	1.1083
FC1-CoRaiS(100)	0.0051	1.4118	0.0051	1.8141	0.0052	1.2704	0.0051	1.7481
FC2-CoRaiS(100)	0.0051	1.4131	0.0052	1.8163	0.0051	1.2703	0.0052	1.7491
FC3-CoRaiS(100)	0.0051	1.4124	0.0052	1.8182	0.0052	1.2704	0.0051	1.7463
CoRaiS(100)	0.0051	1.0221	0.0052	1.0267	0.0052	1.0091	0.0051	1.0361
FC1-CoRaiS(1k)	0.0050	1.2956	0.0052	1.6274	0.0052	1.1837	0.0053	0.8769
FC2-CoRaiS(1k)	0.0051	1.2913	0.0052	1.6269	0.0052	1.1857	0.0051	1.5858
FC3-CoRaiS(1k)	0.0051	1.2929	0.0051	1.6276	0.0052	1.1856	0.0051	1.5851
CoRaiS(1k)	0.0051	1.0148	0.0052	1.0186	0.0052	1.0069	0.0051	1.0297
Gurobi(0.005s)	(44.81%) (1.7981)		(19.69%) (2.6884)		(6.02%) (1.184)		(5.46%) -	
Gurobi(0.01s)	(83.82%) (1.2584)		(45.91%) (2.0371)		(34.91%) (1.3904)		(3.40%) -	
Gurobi(0.05s)	0.0584	1.0009	0.0886	1.0026	0.0629	1.0013	0.1211	1.0334

CoRaiS is trained from 40000 batches on the device with 2×Intel(R) Xeon(R) Gold 5215 CPU that can provide 40 processors and 2×NVIDIA GTX 2080Ti, and *CoRaiS* uses Adam optimizer, PyTorch 1.11 framework and python 3.8 on Ubuntu 18.04.

Baselines It must be mentioned that as our best knowledge, *CoRaiS* is the first artificial intelligence based work that breaks many assumptions of prior works, deals with a multi-edge computing system where every edge is allowed to receive requests from clients, and optimizes an objective function that minimize the responding time over all requests. In order to evaluate the performance of *CoRaiS*, the results generated by *CoRaiS* are compared with that produced by exact solver (*Gurobi*). *Gurobi* is able to help calculate exact solutions. Meanwhile, we propose two heuristic approaches (*Local* and *Random*) as the heuristic baselines in the scenario. Three learning-based baselines are designed as well.

- *Exact baseline*: *Gurobi* is one of the state-of-the-art solver for integer linear programming problems. However, *Gurobi* may fall into long-term calculation due to the huge search space of multi-edge scheduling. Therefore, it is necessary to give a computation time limitation (*x s*).
- *Heuristic baselines*: two algorithms are used to provide heuristic baselines. (i) *Local*: executing all requests at their source locations. (ii) *Random*: randomly sampling the execution edges for all requests. It is allowed to sample multiple times and report the best one.
- *Learning-based baselines (ablation studies for aligning*

modules of CoRais): three synthetic neural network models are used to illustrate the effectiveness of *CoRaiS*. (i) *FC1-CoRaiS*: replacing multi-head attention aligning mechanism of *edge encoder* in *CoRaiS* with multi-layer perceptron, and maintaining the same number of neuron parameters. (ii) *FC2-CoRaiS*: adopting the similar MoD architecture with *CoRaiS*, but using multi-layer perceptron to replace the multi-head attention aligning mechanism in *request encoder*. (iii) *FC3-CoRaiS*: adopting MoD structure, but without aligning mechanisms in both *edge encoder* and *request encoder*, only using multi-layer perceptron to embed edges features and requests features. Since *FC1-CoRaiS*, *FC2-CoRaiS* and *FC3-CoRaiS* adopt the similar MoD architecture and have the same input/output with *CoRaiS*, they are able to use the same decoding strategies with *CoRaiS* as well.

Performance indexes Two indexes are used to evaluate performance. (i) *Time(s)*: time taken to make scheduling decisions, because the multi-edge cooperative computing system needs an approach that can provide a real-time scheduling decision. (ii) *Gap*: quality difference of solutions that are generated by *CoRaiS* and other baselines, compared with the solution generated by *Gurobi(10s)* in the same instance. Solutions from *Gurobi(10s)* are considered as the optimal benchmark in the simulations. The *gap* is computed by (22). \aleph includes *CoRaiS* and other baselines. π signifies the best solution obtained from the specific approach *b* ($b \in \aleph$). $\hat{\pi}$ refers to the best solution generated by *Gurobi(10s)*. $L(\pi)$ refers

TABLE III
GENERALIZATION TEST RESULTS

(*CoRaiS* IS TRAINED ON SMALL-SCALE INSTANCES (EN=10, RN=100) AND DIRECTLY APPLIED INTO LARGER-SCALE INSTANCES. *Time(s)* AND *Gap*: THE LOWER THE BETTER).

Method	EN=10, RN=200		EN=30, RN=400		EN=50, RN=600		EN=50, RN=800	
	Time(s)	Gap	Time(s)	Gap	Time(s)	Gap	Time(s)	Gap
Gurobi(10s)	2.8447	1	3.6902	1	4.0671	1	7.2515	1
Gurobi(0.01s)	(0.09%)	-	0%	-	0%	-	0%	-
Gurobi(0.02s)	(2.99%)	-	0%	-	0%	-	0%	-
Gurobi(0.2s)	0.3235	1.0021	(9.89%)	-	0%	-	0%	-
CoRaiS(greedy)	0.0077	1.3107	0.0119	1.6025	0.0162	1.8897	0.0165	2.3572
CoRaiS(1k)	0.0074	1.0867	0.0118	1.09	0.0159	1.0793	0.0161	1.1954
CoRaiS(10k)	0.0074	1.0752	0.0119	1.0788	0.0161	1.0683	0.0166	1.1720

TABLE IV

CHARACTERISTICS VALIDATION RESULTS

(*CoRaiS* IS TRAINED ON SCHEDULING PROBLEMS (EN=5 AND RN=100). *CoRaiS(1k)* IS USED TO SAMPLE NEAR-OPTIMAL SOLUTIONS. *LB*: LOAD BALANCING; *WP*: WORKLOAD PERCEPTION; *HA*: HETEROGENEITY AWARENESS; *EReqN*: THE NUMBER OF REQUESTS THAT ARE EXECUTED AT EACH EDGES; *LCost*: THE CORRESPONDING RESPONSE TIME.

No.	LB		WP		HA	
	EReqN	LCost	EReqN	LCost	EReqN	LCost
A	22.2094	2.7996	11.4865	2.9964	13.1378	2.0203
B	19.4471	2.8274	18.8379	2.9035	14.9200	2.0285
C	19.4511	2.8267	21.5947	2.7351	19.4577	1.9963
D	19.4523	2.8274	23.2921	2.5227	25.7648	1.8249
E	19.4399	2.8259	24.7888	2.1630	26.7197	1.2267

to the predicted response time for all requests in the multi-edge cooperative computing system, and $L(\pi)$ is computed by (19). The *gap* is critical because the multi-edge cooperative computing system also require the real-time approach to produce a high-quality solution.

$$gap_b = \frac{L(\pi|b)}{L(\hat{\pi}|Gurobi(10s))}, \quad \forall b \in \mathcal{N} \quad (22)$$

B. Results Analysis

1) *Analysis of Conventional Test Results*: *CoRaiS* is a lightweight model that has about 4 million learnable parameters. We trained *CoRaiS* on four scales: (EN=5, RN=50), (EN=5, RN=100), (EN=10, RN=50) and (EN=10, RN=100). *EN* and *RN* denote the number of edges and requests respectively. The models occupy 1511M, 1961M, 1539M, and 2057M on a single GTX 2080Ti GPU during training. We test the performance of learned policies on the same scale problems, and the results are shown in Table II.

(i) *Gurobi* can quickly obtain the optimal solutions for small-scale problems, and the average time costs for (EN=5, RN=50), (EN=5, RN=100) and (EN=10, RN=50) are less than 1s. However, as the problem scale becomes larger, such as (EN=10, RN=100), the solving time increases significantly, even sometimes, *Gurobi* spends 10s but only get a sub-optimal solution.

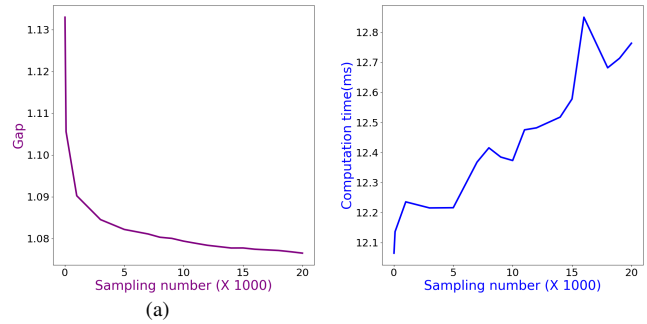


Fig. 7. Testing on 1000 large-scale instances (30 edges and 400 requests) using the *CoRaiS* model trained on the scale with 10 edges and 100 requests. Left: More sampling improves solution quality (gap is decreasing); Right: More sampling slightly increases the computation time.

(ii) The solutions generated by *Gurobi(1s, 10s)* are very close. In practice, *Gurobi* usually uses branch and bound to solve problems. Sometimes it can quickly get a good non-optimal solution, but it will keep exploring in the search space because it wants to obtain a better solution. Therefore, it is difficult to predict the computing time required by *Gurobi* to get a high-quality solution.

(iii) Heuristic approaches (*Local* and *Random*) take near-zero time to give a solution, but the quality is far away from the optimum.

(iv) The solving time taken by *CoRaiS(greedy, 100, 1k)* is close to 0.005s, which is much less than *Gurobi*. The gap closing to 1 shows *CoRaiS* successfully learns an efficient policy that helps produce high-quality solutions. Therefore, *CoRaiS* has potential to provide real-time and high-quality decision to support efficient operations of the multi-edge cooperative computing system.

(v) *CoRaiS* and other three learning-based models (*FC1-CoRaiS*, *FC2-CoRaiS* and *FC3-CoRaiS*) adopt the same decoding strategies (greedy, sampling). The comparison results show that the two alignment mechanisms of edge/request features play important roles in promoting policy learning.

(vi) Because *CoRaiS* spends near 0.005s on solving the problems, we explore the performance of *Gurobi(0.005s)* as well. The experimental results illustrate that it is very difficult

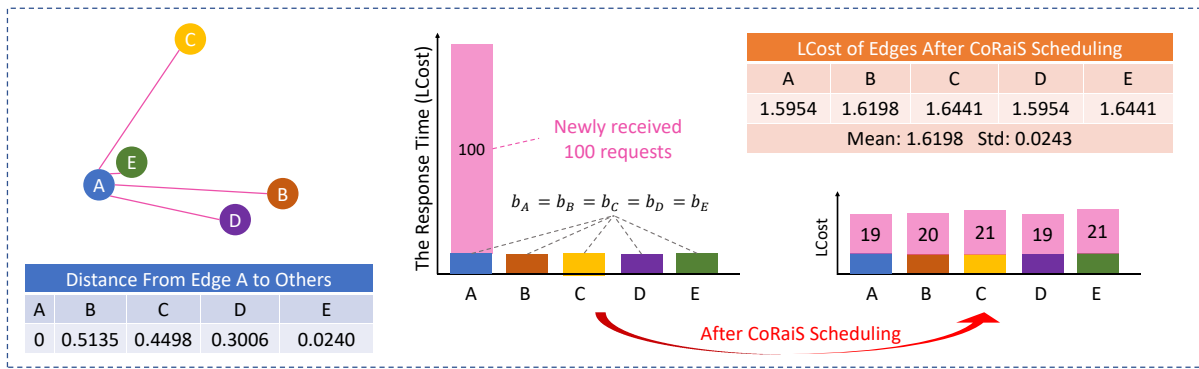


Fig. 8. A case to illustrate that *CoRaiS* learned to optimize scheduling through load balancing without manual intervention. In this case, five edges are homogeneous, i.e. they have same computation time estimation functions. The response times of edges to backlogs are same, i.e. $b_E = b_D = b_C = b_B = b_A$. Since all newly arrived requests are submitted to e_A and will be transferred from e_A , we only depict the relative position relationship between e_A and others in the topology graph at the upper-left part, and quantifies the distance from e_A to others in the table at the lower-left part. The middle graph presents the loads on each edge before being scheduled. The right graph shows the results after *CoRaiS* scheduling. The numbers in the two graphs indicate the number of requests to be executed. The upper-right table predicts the time required for each edge to respond to the scheduled requests.

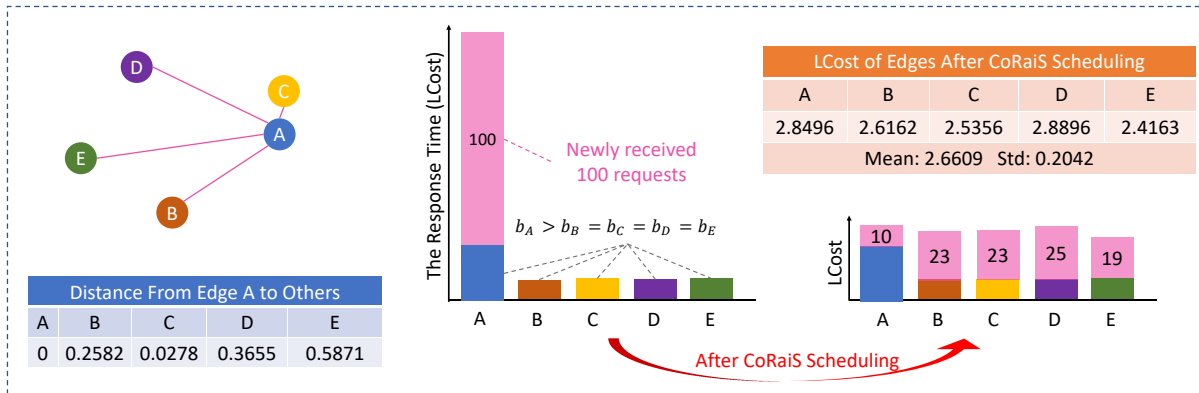


Fig. 9. A case to illustrate that *CoRaiS* is able to perceive workload of edges while scheduling. In this case, five homogeneous edges have same computation time estimation function, but the response times of edges to backlogs satisfy $b_E = b_D = b_C = b_B < b_A$.

for *Gurobi* to solve the problem within such a short time, even to calculate an approximate solution. Then we relax the time constraints to $0.01s$ and $0.05s$. The results generated by *Gurobi(0.01 s)* show that double relaxation does not improve performance much. The proportion of problems that are not solved approximately is still high. Some simple problems can obtain near-optimal solutions, but the solutions are much far from the optimum. The results generated by *Gurobi(0.05s)* shows 10X relaxation helps a lot, since all problems get their sub-optimal solutions. However, the practical calculation time to solve the problems is usually longer than the constraint, such as $0.0886s$ for (EN=10, RN=50) and $0.1211s$ for (EN=10, RN=100), which indicates that *Gurobi* cannot precisely control the solving process according to time constraints, the solving time is still uncontrollable. Moreover, even if the time constraint is relaxed by 10 times, the performance still shows significant degradation when encountering large-scale problems, such as the average gap is 1.0334 for large-scale problems (EN=10, RN=100), while the average gap is 1.0009 for small-scale problems (EN=5, RN=50). Compared with that, *CoRaiS* stabilized the solving time consumption at $0.005s$, meanwhile, the gap increasing from 1.0148 to 1.0297 keeps relatively stable.

2) *Analysis of Generalization Test Results:* We train *CoRaiS* on instances under problem scale setting (EN=10, RN=100). The learned model is directly applied into larger-scale instances. The results are presented in Table III. *Gurobi(10s)* takes a long time ($> 2s$ for average) to compute a good solution and its time cost increases as the problem scale becomes larger, from $2.8s$ for (EN=10, RN=200) to $7.2s$ for (EN=50, RN=800). Compared with *Gurobi(10s)*, *CoRaiS* costs a shorter time ($< 0.02s$) to obtain a high-quality near-optimal solution by sampling, and its time cost does not increase significantly, from $7ms$ for (EN=10, RN=200) to $16ms$ for (EN=50, RN=800), even though the problem scale becomes 20 times larger. We force *Gurobi* to provide solutions within ($< 0.01s$) and ($< 0.02s$) respectively, to check whether it can get similar performance with *CoRaiS*. The results presented in Table III show that *Gurobi* can hardly solve large-scale problems within a short time. Then we relax the time limitation to 10 times, i.e. $0.2s$, the comparison results show that only a few large-scale problems can be solved.

Sampling decoding effect We found that sampling more from the policy generated by *CoRaiS* can improve the solution quality while slightly increasing computation time (at $0.0001s$ level), the experimental results are presented in Fig. 7. *It*

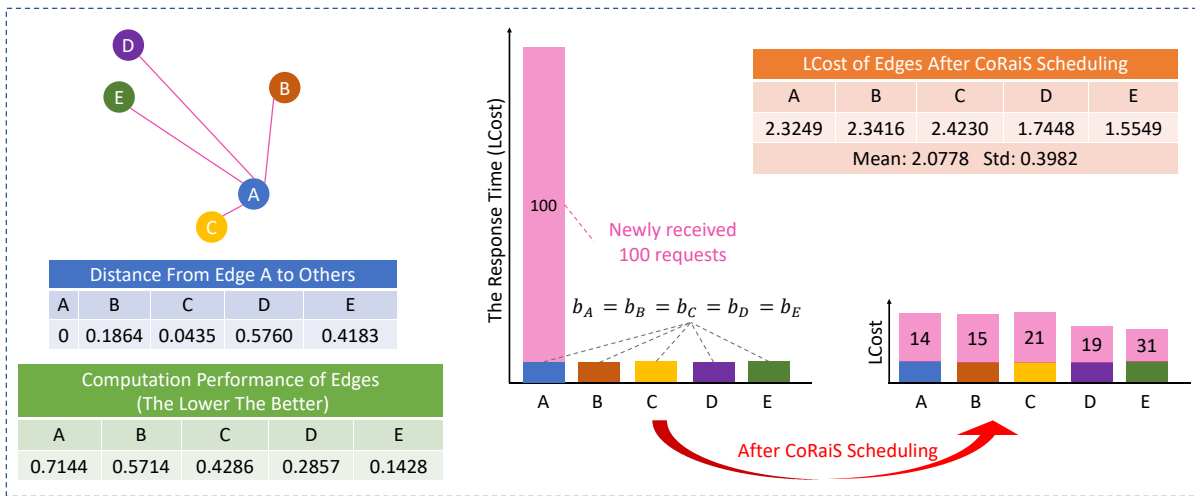


Fig. 10. A case to demonstrate that *CoRaiS* is able to recognize heterogeneity when cooperating multiple edges. In this case, the computing performance of five heterogeneous edges follows the order $E > D > C > B > A$, and the response times of the edges to their backlogs are same.

indicates that *CoRaiS* has the potential to be applied to other multi-edge cooperative computing systems, regardless of their scale, since *CoRaiS* is capable of generating high-quality solution in real-time through sampling.

3) *Analysis of Characteristic Validation Results*: (i) **Load balancing (LB)**: We design five homogeneous edges and push same backlogs on them, so that the initial system-level state of edges are same, and the time of edges responding to backlogs satisfies $b_E = b_D = b_C = b_B = b_A$. Then we conduct 10k experiments on the system. In each experiment, 100 same requests are submitted to e_A , and *CoRaiS* is used to provide a scheduling solution. The results are presented in Table IV(LB). One randomly sampled case shown in Fig. 8 is used to visualize the *CoRaiS* scheduling results. The number of requests executed at five edges are approximately equal, and the response time are very close. Therefore, we claim that *CoRaiS* learned to optimize scheduling through load balancing without manual intervention.

(ii) **Workload perception (WP)**: We design five homogeneous edges and induce differences in response time to backlogs by pushing different numbers of requests to each edge, so that the initial system-level state of edges are different. The time of edges responding to backlogs satisfies $b_E \leq b_D \leq b_C \leq b_B < b_A$. Then 10k experiments submitting 100 requests to e_A are conducted. *CoRaiS* makes decisions to schedule requests. As shown in Table IV(WP), the number of requests to be dispatched to each edge is different and follows the order $n_E \geq n_D \geq n_C \geq n_B > n_A$ on average. Meanwhile, there is no significant difference in response time after scheduling. Fig. 9 visualizes a case to illustrate the workload perception of *CoRaiS*. In this case, since e_A has much heavier original workload than other edges, it keeps a small amount of the newly arrived requests and diverted most of them to speed up the completion of all requests. Therefore, we claim *CoRaiS* is able to perceive workload of edges while scheduling.

(iii) **Heterogeneity awareness (HA)**: We design five heterogeneous edges, that is, the computation time estimation

functions of edges are different. We arrange the computing performance of edges in the order of $E > D > C > B > A$. Then we equalize the response times of the edges to backlogs by adjusting the number of requests. After that, 10k experiments are conducted. In each experiment, 10k same requests are submitted to e_A , and *CoRaiS* is used to provide a scheduling solution. According to the results in Table IV(HA), the more powerful edge serves more requests, and the corresponding response time of all edges are very close. We visualize a randomly sampled illustration in Fig. 10 as well. In this case, e_E responds to the most requests while e_A achieves the fewest, because the computation performance of e_E is much more powerful than that of e_A . With *CoRaiS* scheduling, the variance of estimated responding time of such five edges is very small. Therefore, we claim *CoRaiS* is able to recognize heterogeneity while cooperating multi-edges.

VI. CONCLUSION

The system-level state evaluation model is introduced in this paper, to shield edges heterogeneity in hardware configuration and redefine the service capacity at edges. After that, an integer linear programming formulation is presented for the multi-edge scheduling problem. *CoRaiS*, a learning-based lightweight real-time scheduler, is proposed to minimize the response time over all distributed arriving requests. The experimental results demonstrate that *CoRaiS* successfully learned a strong policy to make high-quality scheduling in real time, irrespective of request arrival patterns and system scales.

REFERENCES

[1] Y. Mao, C. You, J. Zhang, K. Huang, and K. B. Letaief, "A survey on mobile edge computing: The communication perspective," *IEEE communications surveys & tutorials*, vol. 19, no. 4, pp. 2322–2358, 2017.

[2] P. Mach and Z. Becvar, "Mobile edge computing: A survey on architecture and computation offloading," *IEEE communications surveys & tutorials*, vol. 19, no. 3, pp. 1628–1656, 2017.

- [3] V. Farhadi, F. Mehmeti, T. He, T. F. La Porta, H. Khamfroush, S. Wang, K. S. Chan, and K. Poularakis, "Service placement and request scheduling for data-intensive applications in edge clouds," *IEEE/ACM Transactions on Networking*, vol. 29, no. 2, pp. 779–792, 2021.
- [4] Y. Han, S. Shen, X. Wang, S. Wang, and V. C. Leung, "Tailored learning-based scheduling for kubernetes-oriented edge-cloud system," in *IEEE INFOCOM 2021-IEEE Conference on Computer Communications*. IEEE, 2021, pp. 1–10.
- [5] Y. Ren, S. Shen, Y. Ju, X. Wang, W. Wang, and V. C. Leung, "Edgematrix: A resources redefined edge-cloud system for prioritized services," in *IEEE INFOCOM 2022-IEEE Conference on Computer Communications*. IEEE, 2022, pp. 610–619.
- [6] Y. Gao, L. Chen, and B. Li, "Spotlight: Optimizing device placement for training deep neural networks," in *International Conference on Machine Learning*. PMLR, 2018, pp. 1676–1684.
- [7] A. Mirhoseini, A. Goldie, H. Pham, B. Steiner, Q. V. Le, and J. Dean, "A hierarchical model for device placement," in *International Conference on Learning Representations*, 2018.
- [8] J. Chen, P. Han, Y. Zhang, T. You, and P. Zheng, "Scheduling energy consumption-constrained workflows in heterogeneous multi-processor embedded systems," *Journal of Systems Architecture*, vol. 142, p. 102938, 2023.
- [9] X. Ma, A. Zhou, S. Zhang, and S. Wang, "Cooperative service caching and workload scheduling in mobile edge computing," in *IEEE INFOCOM 2020-IEEE Conference on Computer Communications*. IEEE, 2020, pp. 2076–2085.
- [10] C. Yi, J. Cai, T. Zhang, K. Zhu, B. Chen, and Q. Wu, "Workload re-allocation for edge computing with server collaboration: A cooperative queueing game approach," *IEEE Transactions on Mobile Computing*, 2021.
- [11] M. Kumar, S. C. Sharma, A. Goel, and S. P. Singh, "A comprehensive survey for scheduling techniques in cloud computing," *Journal of Network and Computer Applications*, vol. 143, pp. 1–33, 2019.
- [12] L. F. Bittencourt, A. Goldman, E. R. Madeira, N. L. da Fonseca, and R. Sakellariou, "Scheduling in distributed systems: A cloud computing perspective," *Computer science review*, vol. 30, pp. 31–54, 2018.
- [13] A. Arunarani, D. Manjula, and V. Sugumaran, "Task scheduling techniques in cloud computing: A literature survey," *Future Generation Computer Systems*, vol. 91, pp. 407–415, 2019.
- [14] T. He, H. Khamfroush, S. Wang, T. La Porta, and S. Stein, "It's hard to share: Joint service placement and request scheduling in edge clouds with sharable and non-sharable resources," in *2018 IEEE 38th International Conference on Distributed Computing Systems (ICDCS)*. IEEE, 2018, pp. 365–375.
- [15] K. Poularakis, J. Llorca, A. M. Tulino, I. Taylor, and L. Tassiulas, "Joint service placement and request routing in multi-cell mobile edge computing networks," in *IEEE INFOCOM 2019-IEEE Conference on Computer Communications*. IEEE, 2019, pp. 10–18.
- [16] H. Tan, Z. Han, X.-Y. Li, and F. C. Lau, "Online job dispatching and scheduling in edge-clouds," in *IEEE INFOCOM 2017-IEEE Conference on Computer Communications*. IEEE, 2017, pp. 1–9.
- [17] Z. Han, H. Tan, X.-Y. Li, S. H.-C. Jiang, Y. Li, and F. C. Lau, "Ondisc: Online latency-sensitive job dispatching and scheduling in heterogeneous edge-clouds," *IEEE/ACM Transactions on Networking*, vol. 27, no. 6, pp. 2472–2485, 2019.
- [18] H. Mao, M. Schwarzkopf, S. B. Venkatakrishnan, Z. Meng, and M. Alizadeh, "Learning scheduling algorithms for data processing clusters," in *Proceedings of the ACM special interest group on data communication*, 2019, pp. 270–288.
- [19] X. Ni, J. Li, M. Yu, W. Zhou, and K.-L. Wu, "Generalizable resource allocation in stream processing via deep reinforcement learning," in *Proceedings of the AAAI Conference on Artificial Intelligence*, vol. 34, no. 01, 2020, pp. 857–864.
- [20] A. Mirhoseini, H. Pham, Q. V. Le, B. Steiner, R. Larsen, Y. Zhou, N. Kumar, M. Norouzi, S. Bengio, and J. Dean, "Device placement optimization with reinforcement learning," in *International Conference on Machine Learning*. PMLR, 2017, pp. 2430–2439.
- [21] O. Vinyals, M. Fortunato, and N. Jaitly, "Pointer networks," in *Advances in Neural Information Processing Systems*, 2015, pp. 2692–2700.
- [22] Y. Hu, Z. Zhang, Y. Yao, X. Huyan, X. Zhou, and W. S. Lee, "A bidirectional graph neural network for traveling salesman problems on arbitrary symmetric graphs," *Engineering Applications of Artificial Intelligence*, vol. 97, p. 104061, 2021.
- [23] M. Nazari, A. Oroojlooy, L. Snyder, and M. Takác, "Reinforcement learning for solving the vehicle routing problem," in *Advances in Neural Information Processing Systems*, 2018, pp. 9839–9849.
- [24] W. Kool, H. Van Hoof, and M. Welling, "Attention, learn to solve routing problems!" *International Conference on Learning Representations*, 2018.
- [25] M. Kim, J. Park *et al.*, "Learning collaborative policies to solve np-hard routing problems," *Advances in Neural Information Processing Systems*, vol. 34, pp. 10418–10430, 2021.
- [26] Y. Hu, Y. Yao, and W. S. Lee, "A reinforcement learning approach for optimizing multiple traveling salesman problems over graphs," *Knowledge-Based Systems*, vol. 204, p. 106244, 2020.
- [27] E. Khalil, H. Dai, Y. Zhang, B. Dilkina, and L. Song, "Learning combinatorial optimization algorithms over graphs," in *Advances in Neural Information Processing Systems*, 2017, pp. 6348–6358.
- [28] Z. Li, Q. Chen, and V. Koltun, "Combinatorial optimization with graph convolutional networks and guided tree search," in *Advances in Neural Information Processing Systems*, 2018, pp. 539–548.
- [29] N. Sonnerat, P. Wang, I. Ktena, S. Bartunov, and V. Nair, "Learning a large neighborhood search algorithm for mixed integer programs," *arXiv preprint arXiv:2107.10201*, 2021.
- [30] Y. Wu, W. Song, Z. Cao, and J. Zhang, "Learning large neighborhood search policy for integer programming," *Advances in Neural Information Processing Systems*, vol. 34, pp. 30075–30087, 2021.
- [31] M. Wortsman, G. Ilharco, S. Y. Gadre, R. Roelofs, R. Gontijo-Lopes, A. S. Morcos, H. Namkoong, A. Farhadi, Y. Carmon, S. Kornblith, and L. Schmidt, "Model soups: averaging weights of multiple fine-tuned models improves accuracy without increasing inference time," in *Proceedings of the 39th International Conference on Machine Learning*, ser. Proceedings of Machine Learning Research, K. Chaudhuri, S. Jegelka, L. Song, C. Szepesvari, G. Niu, and S. Sabato, Eds., vol. 162. PMLR, 17–23 Jul 2022, pp. 23965–23998. [Online]. Available: <https://proceedings.mlr.press/v162/wortsman22a.html>
- [32] C. Li, L. Li, Y. Geng, H. Jiang, M. Cheng, B. Zhang, Z. Ke, X. Xu, and X. Chu, "Yolov6 v3. 0: A full-scale reloading," *arXiv preprint arXiv:2301.05586*, 2023.
- [33] C. Li, L. Li, H. Jiang, K. Weng, Y. Geng, L. Li, Z. Ke, Q. Li, M. Cheng, W. Nie *et al.*, "Yolov6: A single-stage object detection framework for industrial applications," *arXiv preprint arXiv:2209.02976*, 2022.
- [34] A. Vaswani, N. Shazeer, N. Parmar, J. Uszkoreit, L. Jones, A. N. Gomez, Ł. Kaiser, and I. Polosukhin, "Attention is all you need," *Advances in neural information processing systems*, pp. 5998–6008, 2017.
- [35] C. R. Qi, H. Su, K. Mo, and L. J. Guibas, "Pointnet: Deep learning on point sets for 3d classification and segmentation," in *Proceedings of the IEEE conference on computer vision and pattern recognition*, 2017, pp. 652–660.
- [36] K. Xu, W. Hu, J. Leskovec, and S. Jegelka, "How powerful are graph neural networks?" *International Conference on Learning Representations*, 2019.



Yujiao Hu (Member, IEEE) received her Bachelor and PhD degrees from the Department of Computer Science of Northwestern Polytechnical University, Xi'an, China, in 2016 and 2021 respectively. From Nov. 2018 to March 2020, she was a visiting PhD student in National University of Singapore. Currently, she is a faculty member in Purple Mountain Laboratories. She focuses on deep learning, edge computing, multi-agent cooperation problems and time sensitive networks.



Qingmin Jia is currently a Researcher in Future Network Research Center of Purple Mountain Laboratories. He received the B.S. degree from Qingdao University of Technology in 2014, and received the Ph.D. degree from Beijing University of Posts and Telecommunications (BUPT) in 2019. His current research interests include edge computing, edge intelligence, IoT and future network architecture. He has served as a Technical Program Committee Member of IEEE GLOBECOM 2021, HotICN 2021.



Renchao Xie received the Ph.D. degree from the School of Information and Communication Engineering, Beijing University of Posts and Telecommunications (BUPT), Beijing, China, in 2012. He is a Professor with BUPT. From July 2012 to September 2014, he worked as a Postdoctoral Fellow with China United Network Communications Group Company. From November 2010 to November 2011, he visited Carleton University, Ottawa, ON, Canada, as a Visiting Scholar. His current research interests include 5G network and edge computing, information-centric networking, and future network architecture. Dr. Xie has served as a Technical Program Committee Member of numerous conferences, including IEEE Globecom, IEEE ICC, EAI Chinacom, and IEEE VTC-Spring.



Jinchao Chen is an associate professor at School of Computer Science in Northwestern Polytechnical University, Xi'an, China. He has received his Ph.D. degree in Computer Science from the same institution in 2016. His interest includes the multi-agent cooperation, real-time system, cloud computing.



Yuan Yao is currently an Associate Professor in the School of Computer Science, Northwestern Polytechnical University (NPU). He received the B.S. M.S., and Ph.D. degrees in computer science from Northwestern Polytechnical University, Xi'an, China, in 2007, 2009 and 2015, respectively. He was a Postdoctoral Researcher in the Department of Computing at Polytechnic University, Hong Kong from 2016 to 2018. His research interests are in the area of real-time and embedded systems, swarm intelligence operating systems and cyber physical

system.



F. Richard Yu received the Ph.D. degree in electrical engineering from the University of British Columbia, Vancouver, BC, Canada, in 2003. From 2002 to 2006, he was with Ericsson, Lund, Sweden, and a start-up in California, USA. He joined Carleton University, Ottawa, ON, Canada, in 2007, where he is currently a Professor. His research interests include wireless cyber-physical systems, connected/autonomous vehicles, security, distributed ledger technology, and deep learning. He is a Distinguished Lecturer, the Vice President (Membership), and an Elected Member of the Board of Governors of the IEEE Vehicular Technology Society. He is a Fellow of the IEEE, Canadian Academy of Engineering (CAE), Engineering Institute of Canada (EIC), and Institution of Engineering and Technology (IET).



Yan Pan is currently a lecture at the Science and Technology on Information Systems Engineering Laboratory, National University of Defense Technology, Changsha, China, since Dec. 2020. Before that, he respectively received the B.S. degree in 2013 and the Ph.D. degree in 2021 from Northwestern Polytechnical University, Xi'an, China. He was a visiting student to University of Maryland, United States, during Jan. 2017 and Nov. 2018. His research interests include Industrial Internet of Things, industrial robots, and edge computing.